Δελτίο της Ελληνικής Γεωλογικής Εταιρίας, τομ. XLVII , 2013
Πρακτικά 13ου Διεθνούς Συνεδρίου, Χανιά, Σεπτ. 2013

Bulletin of the Geological Society of Greece, vol. XLVII 2013
Proceedings of the 13th International Congress, Chania, Sept. 2013

TIME SERIES ANALYSIS OF THE NOANET CGPS STATIONS

Chousianitis K.[1], Ganas A.[1], Papanikolaou M.[1], Argyrakis P.[1], Drakatos G.[1] and Makropoulos K.[1]

[1] Institute of Geodynamics, National Observatory of Athens, chousianitis@noa.gr, aganas@noa.gr, g.drakat@noa.gr, papanikolaou@geol.uoa.gr,pargyrak@geol.uoa.gr, kmacrop@geol.uoa.gr

Abstract

The National Observatory of Athens has begun installing permanent GPS stations on February 2006 including a EUREF permanent station in Attica, NOA1. Currently the National Observatory of Athens operates 20 continuous GPS stations around Greece all sampling at 1-s and transmitting real-time data to Athens. Several stations also sample at 0.2-s (5 Hz) and record the data in the ring buffer for a period of 1-2 days. Their location is carefully selected so that both geological and seismotectonic criteria are fulfilled. All stations are situated close to major seismogenic structures of Greece such as the Cephalonia Transform Fault (CTF) in the Ionian Sea (VLSM, PONT, SPAN, KIPO), and the two North Anatolian Fault branches in the North Aegean Sea (PRKV, LEMN). We describe the CGPS data archiving and processing procedures, used to combine into a uniform velocity solution the observations of all the NOANET stations, accounting for the seasonal (annual and semi-annual) signals, and considering the off-sets in the coordinate time-series.
Key words: *Geodesy, Geodynamics, Time series analysis, Greece.*

Περίληψη

Το Γεωδυναμικό Ινστιτούτο του ΕΑΑ ξεκίνησε γεωδαιτικές παρατηρήσεις το έτος 2006 με την ίδρυση και λειτουργία του μονίμου σταθμού αναφοράς NOA1. Σήμερα το δίκτυο NOANET αριθμεί 20 μόνιμους σταθμούς (σε συνεργασία με τρίτους φορείς) με βήμα δειγματοληψίας το 1-s και σε σύνδεση πραγματικού χρόνου με το κέντρο συλλογής και αποθήκευσης των δεδομένων (Αθήνα, Θησείο). Αυτή η εργασία παρουσιάζει την διαδικασία συλλογής και επεξεργασίας των δεδομένων GPS, λαμβάνοντας υπόψη τα περιοδικά σήματα (ετήσια και ημιετήσια) που υπεισέρχονται στις χρονοσειρές και δίνοντας σφάλματα στις εκτιμήσεις των ταχυτήτων με ανάλυση ενός μοντέλου θορύβου. Τέλος, παρουσιάζονται αποτελέσματα στο ITRF2005 για τους σταθμούς εκείνους των οποίων η διάρκεια καταγραφής έχει ξεπεράσει τα τρία χρόνια, γεγονός που εξασφαλίζει αξιόπιστες τιμές ταχυτήτων.
Λέξεις κλειδιά: *Γεωδαισία, Γεωδυναμική, Ανάλυση χρονοσειρών, Ελλάδα.*

1. Introduction

Greece is located at a complex seismotectonic regime dominated by the convergence of Mediterranean and Eurasian plates and their collision along the Hellenic Arc. As a result the area exhibits high seismicity. Relative motion of these plates accumulates stress in the lithosphere,

causing observable crustal deformation (McClusky et al., 2000; Ganas and Parsons, 2009; Floyd et al., 2010). Earthquake activity occurs due to tectonic stress release along both, the crustal faults and the Mediterranean-Eurasia plates' interface, a fact that makes the study of crustal deformation an interesting and essential issue. In southern Greece, earthquakes are caused primarily by interaction between the relatively small Aegean Sea and the larger Africa (Nubia) plates. In northern Greece the main seismic hazard comes from the two branches of the north Anatolian Fault that terminate inside the Aegean Sea. In western Greece there are two large faults, both offshore, the Cephalonia Transform and the Appulian thrust. The largest 20th earthquakes to have occurred near Greece's plate boundaries had magnitudes of about 7.2-7.3. However, globally, convergent-plate tectonic environments similar to that of the Hellenic arc commonly produce M>8 earthquakes.

Geodetic investigation of the kinematics of Greece via campaign GPS observations started in the late 1980s – early 1990s following the documentation of large-scale continental extension across the Gulf of Corinth (~1 cm/yr; Billiris et al., 1991). It was soon realized that the kinematics of deformation involved a combination of westerly motion of Anatolia and south-westerly motion of the central and south Aegean, relative to Eurasia, in tandem with N-S convergence across the Hellenic Arc (Le Pichon et al., 1995; McClusky et al., 2000; Kahle et al., 2000). It is also evident that there is a progressive increase in GPS velocities southward in northern Greece (Macedonia – Thrace) toward the North Aegean Trough, across which the velocities increase and change direction dramatically. During the last decade, a number of groups conducted research on the fragmentation of the upper crust in microplates or continental blocks (e.g. Avallone et al., 2004; Nyst and Thatcher, 2004; Reilinger et al., 2006; Floyd et al., 2010) and on mapping crustal motions and interseismic velocities in the central part of the country (e.g. Briole et al., 2000; Bernard et al., 2006; Hollenstein et al., 2008). Most of above studies show that present-day Aegean deformation is typically focused in narrow deforming zones (rift axes or transcurrent faults) that are surrounded by rigid, less active blocks. The Institute of Geodynamics of the National Observatory of Athens, in order to monitor the ongoing deformation across major fault zones in Greece and to correlate the rate of strain accumulation with the occurrence of major earthquakes, has began the installation since 2006 of NOANET, a real-time, high-rate GNSS network. This paper describes the instrumental set-up, the data-logging strategy and the processing procedures used to combine into a uniform velocity solution the observations of the NOANET continuous GPS (CGPS) network.

2. Instrumentation and Data Archiving

The NOANET network currently comprises 20 stations (Figure 1) and has been operating since February 2006 following the EUREF (Regional Reference Frame Sub-Commission for Europe) Permanent Network standards. The aim of this network is to monitor and quantify crustal deformation in Greece, so the location of each station was carefully selected in order that both geological and seismotectonic criteria are fulfilled. Most stations are located close to major seismogenic structures of Greece in order to optimally measure tectonic motions. The stability of points was an important issue during the network design. All stations are installed on bedrock (Table 1).

The NOANET stations are connected to the main server in Athens via the Internet or via leased telephone lines and have 1-week power autonomy. All stations are equipped with dual-frequency GPS receivers. Our stations collect data every 1 s and transmit them to Athens on the hour (hourly files). 5 Hz (0.2 s) data are also collected on the ring buffer and remain available for manual download for a period of 48 hours. Data archiving is performed in two modes: a) 1-s raw data of each station are archived in hourly intervals and b) daily data for each station are archived in 30-s sampling rates. Two diagrams showing 30-s data completeness for NOANET stations since 2006 are presented in Figure 2.

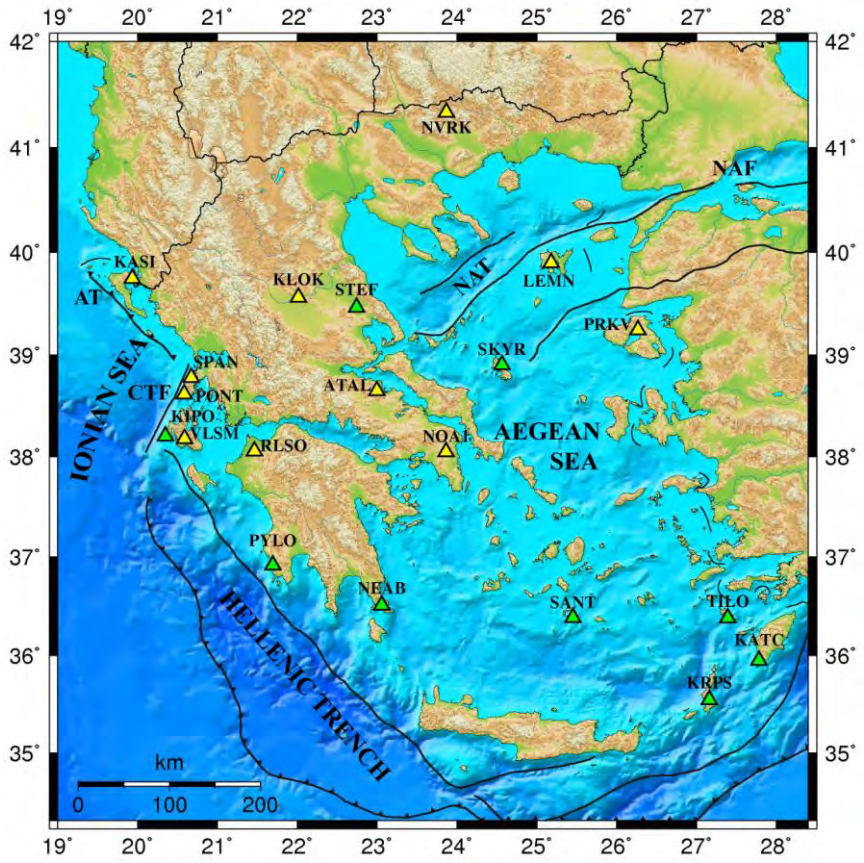

Figure 1 – Relief map showing the locations of the CGPS stations archived at NOA. Yellow triangles denote stations installed prior to 2011. Abbreviations: AT, Apulian Thrust; CTF, Cephalonia Transform Fault; NAT, North Aegean Trough; NAF, North Anatolian Fault.

The network server in Athens is collecting data in automatic mode. The in-house software consists of the LEICA SPIDER sofware version 4.1.1 which is used to manage check and control the reference stations as stand alone stations and as a network. A daily file is created at midnight by sub-sampling the hourly observations every 30-s intervals. This file is converted to RINEX format and delivered to the NOA Web Server where it is available for immediate download (http://www.gein.noa.gr/services/GPS/GPS_DATA/). We currently use a real-time quality processing of four reference stations using the LEICA SpiderQC v.4.1 software.

Table 1 - NOANET station coordinates and monumentation.

Code	Lat.	Long.	Date	Monumentation	Lithology
VLSM	38.177	20.588	2/14/2006	Roof	Limestone
NOA1	38.047	23.864	3/13/2006	Roof	Marble
RLSO	38.056	21.465	7/29/2006	Roof	Sandstone
PONT	38.619	20.585	2/15/2007	Roof	Limestone
KASI	39.746	19.935	4/1/2007	Roof	Limestone
SPAN	38.781	20.673	5/22/2007	Roof	Schist

Code	Lat.	Long.	Date	Monumentation	Lithology
LEMN	39.897	25.181	6/16/2007	Roof	Andesite
PRKV	39.246	26.265	6/30/2007	Exposed Rock	Andesite
NVRK	41.337	23.870	7/12/2007	Roof	Sandstone
KLOK	39.565	22.014	7/17/2008	Exposed Rock	Marble
ATAL	38.653	22.999	3/27/2009	Roof	Alluvium
KIPO	38.203	20.348	8/31/2010	Roof	Limestone
PYLO	36.914	21.695	8/24/2011	Roof	Limestone
NEAB	36.509	23.060	6/27/2012	Roof	Sandstone
KPRS	35.547	27.162	8/14/2012	Roof	Sandstone
SANT	36.385	25.452	8/17/2012	Roof	Volcanic Rocks
KATC	35.951	27.781	10/05/2005	Steel mast	Marl
STEF	39.464	22.742	9/7/2012	Roof	Conglomerate
SKYR	38.904	24.565	11/27/2012	Roof	Schist
TILO	36.380	27.394	07/01/2005	Exposed Rock	Limestone

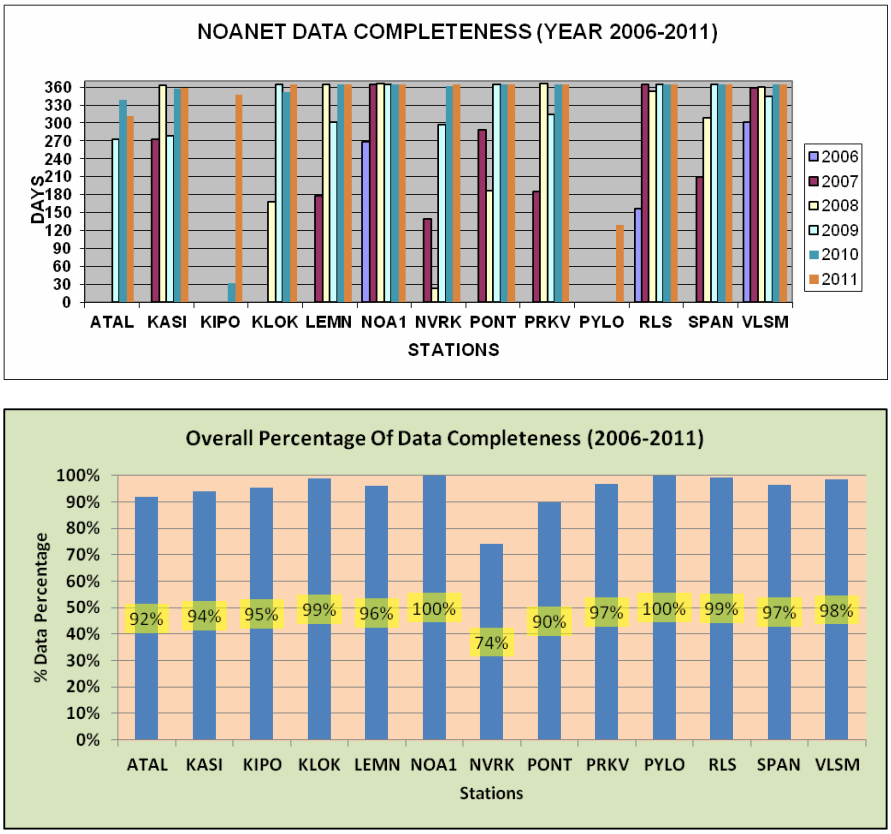

Figure 2 - Diagrams of NOANET data completeness from 2006 until 2011.

3. Processing of CGPS Data

All data are processed in 24-h sessions using the GAMIT/GLOBK software package (Version 10.4; Herring et al., 2010) in a three step distributed processing approach, which is based on the «quasi-observation» theory and the reference frame is not defined until the last step of the analysis (Feigl et al., 1993; Dong et al., 1998). In the first step we apply loose a priori constraints to all of the parameters, choosing the ionosphere-free linear combination, and fixing the ambiguities to integer values to obtain daily estimates of station coordinates, satellite state vectors, the tropospheric zenithal path delay at each station every 2 hr, and the orbital and Earth Orientation parameters (EOP). We use precise orbits from the International GNSS Service (IGS). The effect of solid-earth tides, polar motion and oceanic loading is taken into account according to the IERS/IGS standard 2003 model (McCarthy and Petit, 2004). We apply the ocean-loading model FES2004 (e.g. Lyard et al., 2006) and use IGS absolute elevation and azimuth dependent tables for modeling the effective phase center of the receiver and satellites antennas. Data from 21 well performing fiducial stations of IGS are included in the analysis to tie our regional measurements to an external global reference frame and to improve the ambiguity resolution by putting tight constraints (3 to 5 mm on the horizontal and 5 to 10 mm on the vertical) on these sites from their a priori coordinate values in the ITRF05 Reference Frame (Altamimi et al., 2007). The coordinates of the Greek permanent stations are allowed to vary freely by way of very loose constraints (50 metres). An automatic cleaning algorithm is applied to post-fit residuals in order to repair cycle slips and to remove outliers. For each session, we obtain two solutions based on phase ambiguity resolution, one bias-free and one bias-fixed, along with the associated variance-covariance matrices.

In the second step, we combine our loosely constrained bias-fixed solutions of our regional network with analyzed global and regional solutions provided by SOPAC (http://sopac.ucsd.edu) into single day unconstrained solutions. In the final third step we obtain station position time series in a common reference frame by considering the daily loosely constrained estimates of station coordinates, orbits and EOP and their associated variance-covariance matrices as quasi-observations and passing them to GLOBK which employs the Kalman filtering approach. The reference frame during the formation of these combined network solutions is again loosely defined until the last processing step, where we realize a common reference frame applying generalized constraints (Dong et al., 1998; 2002) while estimating a seven-parameter Helmert transformation (three network rotations, three network translations and one scaling parameter), aligning each individual daily solution to the 2008 realization of the International Terrestrial Reference Frame. The reference frame is defined by minimizing, in the least-square sense, the departure from the prior values determined in the ITRF05-NNR frame of the 21 IGS stations incorporated in the GAMIT processing part. Five iterations are used to eliminate bad sites and to compute station weights for the reference frame stabilization.

3.1. First-order Features of Time Series

After deriving the position time series, we perform an analysis with the aim of modeling the constant velocity for each component of each station, together with the annual and semi-annual signals and the offsets observed in the series using TSVIEW software (Herring, 2003). The successful modeling of these first-order features observed in time series leads to accurate and realistic determination of geodetic velocities. They have been identified in several studies of continuous GPS time series and include seasonal signals and epoch offsets. Seasonal signals may be related to a) gravitational excitation, such as solid Earth tides, ocean tides, and atmospheric tides, b) to thermal origin coupled with hydrodynamics, such as ground water change in both liquid and solid form, and bedrock expansion, and c) to sources that are indirect due to geophysical processes, or of instrument, or modeling deficiency, such as incomplete removal of atmospheric effects and thermal effects of antenna and monument (Blewitt et al., 2001; Van Dam et al., 2001; Blewitt and Lavallee, 2002; Dong et al., 2002). These signals are commonly modeled as a

combination of sinusoids with a fundamental period of one year plus first harmonic mode of six-month period. The epoch offsets in the time series are in general caused either by nearby earthquakes that affect the GPS station, or by antenna changes. The latter can occur when these changes are not well-modeled in the processing software due to erroneous references during the installation time, or when the antenna model does not adequately describe the measurements (Nikolaidis, 2002). The mathematical expression that describes the geodetic time series accounting for first-order features may be written (Langbein, 2004) as:

Equation 1 – Expression for First-order Features Modeling of Time Series

$$d_i = a + bt_i + \sum_{k=1}^{k_0} v_k (t_i - T_k) H(t_i - T_k) + \sum_{j=1}^{j_0} o_j H(t_i - T_j) + \\ + \sum_{m=1}^{m_0} \left[a_m \sin\left(\frac{2\pi t_i}{T_m} \right) + b_m \cos\left(\frac{2\pi t_i}{T_m} \right) \right] + e_i$$

where d_i is the measurement at time t_i; α is the site position; b is the linear rate; v_k are rate changes starting at $t_i=T_k$; $H(t_i-T_j)$ is the Heaviside step function which equals 1 for $t_i \geq T_j$ and 0 otherwise; o_j are offsets in the time series at $t_i=T_j$; α_m and b_m are sine and cosine amplitudes at period T_m and e_i denotes noise.

Moreover, because of the existence of abnormal outliers in daily solutions, we perform editing in order to remove erroneous samples from contaminating the velocity solutions, and to retrieve clean time series. We use an automatic outlier function with a 5 sigma rejection level. As an example, we present the north, east and up raw and detrended position time series, with annual and semi-annual signals and offsets for two NOANET stations in Figure 3a and 3b, respectively. In some time series we detect offsets, which we model as step functions. All these offsets are identified by inspecting the data residuals in combination with the knowledge of each site history and nearby earthquakes. So far, all of the observed offsets in the time series can be attributed to hardware changes within the time span of the processed data apart from the offsets mainly in the North and Up components of RLSO which can be attributed to co-seismic deformation generated by the nearby 2008 Achaia earthquake (Figure 3a; Ganas et al., 2009).

3.2. Error Estimates of Station Velocities

Analyses of continuous GPS data have showed that there is a significant amount of coloured noise content within geodetic time series (e.g. Bock et al., 1997; Zhang et al., 1997). Thus, the white noise assumption that measurement errors are random and uncorrelated from one epoch to its next is not the case for GPS data (e.g. Johnson and Agnew, 1995; Williams et al., 2004) and if a pure white-noise model is used, it may result in unrealistically low velocity uncertainties, especially for continuous data, that can be underestimated by a factor of 5 or more (e.g. Mao et al., 1999). To account for time-correlated errors in our processed time series, we model them using a first-order Gauss-Markov process. For each coordinate component we estimate the increase in the normalized χ^2 (chi-squared per degree of freedom) of successively longer time averages. For a white noise error model, the normalized χ^2 would not depend on averaging time, but for non-white noise spectra, the normalized χ^2 increases with successively increasing averaging time. Next, the time-averaged values of the normalized χ^2 are fitted to the exponential function expected for a first-order Gauss-Markov process so as to estimate a correlation time and the long-term variance. This model is used to predict site velocity uncertainties based on the span of the time series. Since GLOBK is a Kalman filter that is able to realize random walk noise model, which is a first-order Gauss-Markov model with infinite averaging time, we calculate the random walk model values

that would predict the same velocity uncertainties as the first-order Gauss-Markov model for the time series using the following equation:

Equation 2 - Magnitude of Random Walk Noise Component

$$b^2 = \sigma_{RW} T$$

where b is the magnitude of the random walk noise, σ_{RW} is the velocity uncertainty estimates and T is the time span of the time series (Zhang et al., 1997). These values are used as input to GLOBK in order to add random walk to the error model and calculate ‘‘realistic’’ uncertainties for the velocity estimates. After the above time series analysis, our final velocity solution accounting for seasonal signals, offsets and time-correlated noise content is produced by combining the individual epoch-by-epoch solutions into one “stacked” solution by means of the GLOBK's Kalman filter.

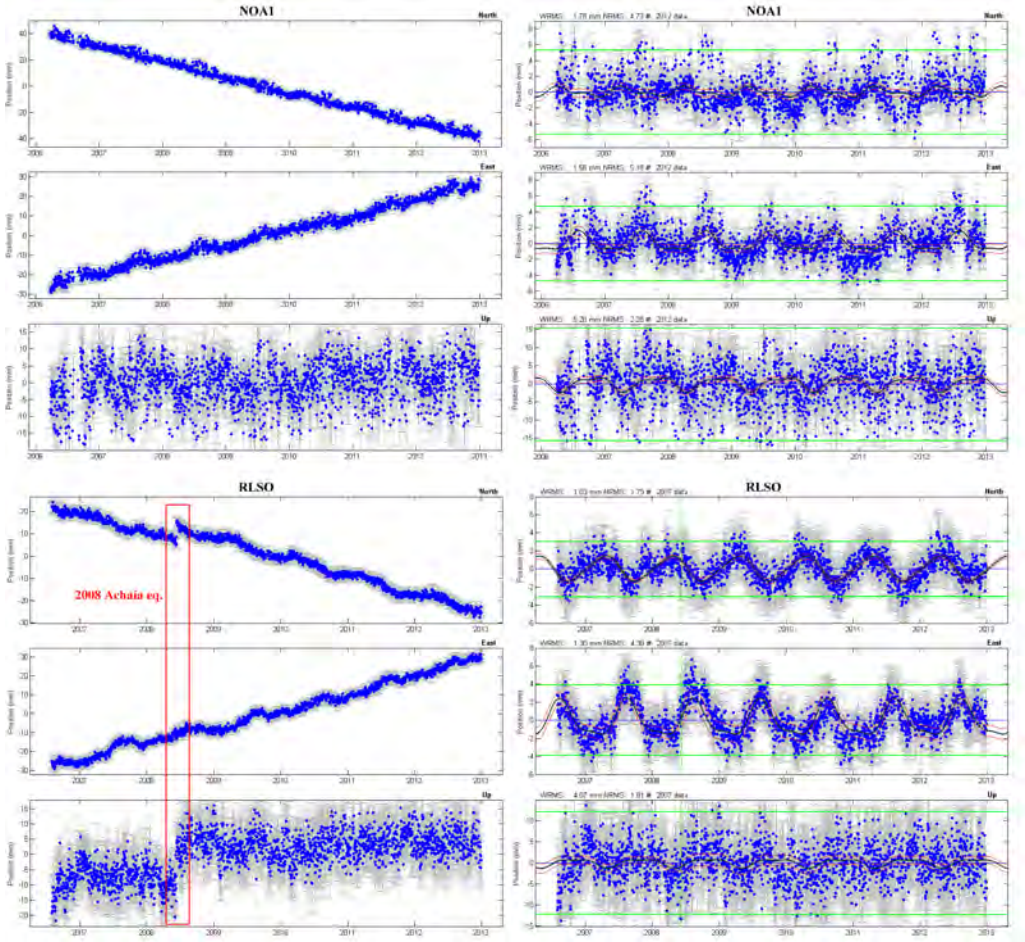

Figure 3 – a) Raw time series plots of daily position estimates of stations NOA1 and RLSO referred to the ITRF2005 reference frame (N, E, U). The error bars represent 1-σ uncertainties obtained from the analysis. b) Detrended time series plots of daily position estimates of stations NOA1 and RLSO referred to the ITRF2005 reference frame (n,e,u). The error bars represent 1-σ uncertainties obtained from the analysis. The black solid lines represent the annual and semi-annual signals along with their uncertainties (red lines, placed plus and minus 1-σ), while the vertical green lines show epochs of detected offsets.

Table 2 - ITRF2005 positions together with velocities and 1-σ uncertainties.

	Position				ITRF2005 Velocity (mm/yr)			White noise/Random Walk Uncertainty (mm/yr)		
Station	**X**	**Y**	**Z**	**Epoch**	**Ve**	**Vn**	**Vu**	**σVe**	**σVn**	**σVu**
NOA1	4599643.3188	2034827.9763	3909890.7492	2011.210	7.16	-11.94	0.82	0.03/0.14	0.03/0.11	0.09/0.24
VLSM	4699991.6109	1765547.7167	3921162.2145	2010.338	17.20	3.67	-0.44	0.03/0.13	0.03/0.16	0.10/0.27
RLSO	4679938.9937	1840151.1569	3910407.7025	2010.391	8.86	-8.58	0.56	0.05/0.41	0.04/0.20	0.16/0.55
LEMN	4434466.0760	2084864.3739	4069305.4627	2009.809	6.56	-1.37	0.86	0.03/0.18	0.04/0.41	0.10/0.26
KASI	4616572.5823	1674415.5562	4056441.2931	2009.664	19.49	14.10	-1.12	0.04/0.08	0.03/0.10	0.12/0.24
KLOK	4564747.0219	1845610.7736	4040935.1159	2009.710	20.74	5.78	-1.07	0.05/0.18	0.04/0.08	0.15/0.41
SPAN	4658312.2345	1757780.6697	3973702.5878	2009.796	20.69	4.01	-0.31	0.04/0.22	0.04/0.30	0.11/0.25
PONT	4671272.6580	1754437.0593	3959389.3952	2009.116	19.53	7.65	-2.78	0.05/0.17	0.03/0.08	0.14/0.51
ATAL	4591113.8365	1948751.1665	3962396.6812	2010.081	12.06	-5.29	0.73	0.10/0.18	0.09/0.23	0.41/1.59
PRKV	4435581.3060	2188830.4885	4013585.9082	2009.732	4.64	-0.14	-0.92	0.10/0.22	0.09/0.25	0.31/0.87

4. Conclusions

In this paper we present the NOANET, a permanent GPS network for regional studies in seismology and geodynamics in Greece. We described the procedures routinely used to download, store and analyze data from NOANET, with the goal of deriving a self-consistent three dimensional velocity field that can be used for further geodynamics and geo-kinematics applications, such as to measure coseismic, postseismic, and interseismic deformation across major fault zones; plate motion and crustal deformation at plate boundaries in the eastern Mediterranean; volcano deformation along the south Aegean Volcanic Arc; and the deformation associated with glacio-eustatic motions and its application to sea-level studies. We produce daily bias-free and bias-fixed solutions of the geodetic parameters along with the associated variance-covariance matrices. We process IGS stations together with the Greek stations in order to optimize the network internal constraints. The daily solutions derived from the processing are characterized by a very high percentage of fixed narrow-lane phase ambiguities up to 95%. Prior to producing the velocity solution, we analyze the time series for periodic signals, offsets, and accounting for time-correlated noise content, because each of these factors affects the velocity estimate and the associated errors (Table 2).

5. Acknowledgments

We thank our colleagues Marco Anzidei, Enrico Serpelloni, Pierre Briole, Bob King, Kirill Palamarchuk and Ivan Georgiev for useful discussions on network operation and data processing. NOANET was funded by EU (FP6 and FP7), regional programmes and Greek Government funds.

6. References

Altamimi Z., Collilieux X., Legrand J., Garayt B. and Boucher C. 2007. ITRF2005: a new release of the International Terrestrial Frame on the time series of station positions and Earth orientation parameters, *J. Geophys. Res.,* 112(B09401), doi:10.1029/2007JB004949.

Avallone A., Briole P., Agatza-Balodimou A.M., Billiris H., Charade O., Mitsakaki C., Nercessian A., Papazissi K., Paradissis D. and Veis G. 2004. Analysis of eleven years of deformation measured by GPS in the Corinth Rift Laboratory area, *C.R. Geoscience*, 336, 301–312.

Bernard P., Lyon-Caen H., Briole P., Deschamps A., Boudin F., Makropoulos K., Papadimitriou

P., Lemeille F., Patau G., Billiris H., Paradissis D., Papazissi K., Castarede H., Charade O., Nercessian A., Avallone A., Pacchiani F., Zahradnik J., Sacks S. and Linde A. 2006. Seismicity, deformation and seismic hazard in the western rift of Corinth: New insights from the Corinth Rift Laboratory (CRL), *Tectonophysics*, 426(1-2), 7–30.

Billiris H., Paradissis D., Veis G., England P., Featherstone W., Parsons B., Cross P., Rands P., Rayson M., Sellers P., Ashkenazi V., Davison M., Jackson J. and Ambraseys N. 1991. Geodetic determination of tectonic deformation in central Greece from 1900 to 1988, *Nature*, 350, 124–129.

Blewitt G., Lavallee D., Clark P. and Nurutdinov K. 2001. A new global mode of Earth deformation: Seasonal cycle detected, *Science*, 294, 2342– 2345.

Blewitt G. and Lavallee D. 2002. Effect of annual signals on geodetic velocity, *J. Geophys. Res.*, 107(B7), 2145, doi:10.1029/2001JB000570.

Bock Y., Wdowinski S., Fang P., Zhang J., Williams S., Johnson H., Behr J., Genrich J., Dean J., Van Domselaar M., Agnew D., Wyatt F., Stark K., Oral B., Hudnut K., King R.W., Herring T.A., Dinardo S., Young W., Jackson D. and Gurtner W. 1997. Southern California permanent GPS geodetic array: Continuous measurements of crustal deformation between the 1992 Landers and 1994 Northridge earthquakes, *J. Geophys. Res.*, 102, 18013–18033.

Briole P., Rigo A., Lyon-Caen H., Ruegg J.C., Papazissi K., Mitsakaki C., Balodimou A., Veis G., Hatzfeld D. and Deschamps A. 2000. Active deformation of the Corinth rift, Greece: Results from repeated Global Positioning System surveys between 1990 and 1995, *J. Geophys. Res.*, 105(B11), doi:10.1029/2000 JB900148.

Dong D.N., Herring T.A. and King R.W. 1998. Estimating regional deformation from a combination of space and terrestrial geodetic data, *J. of Geod.*, 72, 200–214.

Dong D.N., Fang P., Bock Y., Cheng M.K. and Miyazaki S. 2002. Anatomy of apparent seasonal variations from GPS-derived site position time series, *J. Geophys. Res.*, 107(B4), 2075, doi:10.1029/2001JB000573.

Feigl K.L., Agnew D.C., Bock Y., Dong D.N., Donnellan A., Hager B.H., Herring T.A., Jackson D.D., King R.W., Larsen S.K., Larson K.M., Murray M.H. and Shen Z.K. 1993. Measurement of the velocity field in central and southern California, *J. Geophys. Res.*, 98, 21667–21712.

Floyd M.A., Billiris H., Paradissis D., Veis G., Avallone A., Briole P., McClusky S., Nocquet J-M., Palamartchouk K., Parsons B. and England P.C. 2010. A new velocity field for Greece: Implications for the kinematics and dynamics of the Aegean, *J. Geophys. Res.*, 115(B10403), doi:10.1029/2009JB007040.

Ganas A. and Parsons T. 2009. Three-dimensional model of Hellenic Arc deformation and origin of the Cretan uplift, *J. Geophys. Res.*, 114(B06404), doi: 10.1029/2008JB005599.

Ganas A., Serpelloni E., Drakatos G., Kolligri M., Adamis I., Tsimi C. and Batsi E. 2009. The Mw 6.4 SW-Achaia (western Greece) earthquake of 8 June 2008: Seismological, field, GPS observations and stress modeling, *J. Earthquake Eng.*, 13, 1101–1124.

Herring T.A. 2003. MATLAB Tools for viewing GPS velocities and time series, *GPS Solut.*, 7(3), 194–199.

Herring T.A., King, R.W. and McClusky S. 2010. *Documentation for the GAMIT/GLOBK GPS processing software release 10.4.*, Mass. Inst. of Technol., Cambridge.

Hollenstein, C., Müller, M.D., Geiger, A.and Kahle H.G. 2008. Crustal motion and deformation in Greece from a decade of GPS measurements, 1993–2003, *Tectonophysics*, 449, 17–40.

Johnson H. and Agnew D. 1995. Monument motion and measurements of crustal velocities, *Geophys. Res. Lett.*, 22, 2905–2908.

Kahle H-G., Cocard M., Peter Y., Geiger A., Reilinger R., Barka A.and Veis G. 2000. GPS-derived strain rate field within the boundary zones of the Eurasian, African, and Arabian Plates, *J. Geophys. Res.*, 105(B10), 23353–23370.

Langbein J. 2004. Noise in two-color electronic distance meter measurements revisited, *J. Geophys. Res.*, 109(B4), B04406, doi:10.1029/2003JB002819.

Le Pichon X., Chamot-Rooke N., Lallemant S., Noomen R. and Veis G. 1995. Geodetic determination of the kinematics of central Greece with respect to Europe: implications for eastern Mediterranean tectonics, *J. Geophys. Res.*, 100(B7), 12675–12690.

Lyard F., Lefevre F., Letellier T. and Francis O. 2006. Modeling the global ocean tides: modern insights from FES2004, *Ocean Dyn.*, 56(5-6), 394–415, doi:10.1007/s10236-006-0086-x.

Mao A., Harrison C.G.A. and Dixon T.H. 1999. Noise in GPS coordinate time series, *J. Geophys. Res.*, 104, 2797–2816.

McCarthy D.D. and Petit G. 2004. IERS Conventions 2003*, IERS Technical Note*, 32, Verlag des Budesamts fuer Kartographie und Geodasie, Frankfurt.

McClusky S., Balassanian S., Barka A., Demir C., Ergintav S., Georgiev I., Gurkan O., Hamburger M., Hurst, K., Kahle H., Kastens K., Kekelidze G., King R., Kotzev V., Lenk O., Mahmoud S., Mishin A., Nadariya M., Ouzounis A., Paradissis D., Peter Y., Prilepin M., Reilinger R., Sanli I., Seeger H., Tealeb A., Toksoz M.N. and Veis G. 2000. Global Positioning System constraints on plate kinematics and dynamics in the eastern Mediterranean and Caucasus, *J. Geophys. Res.*, 105(B3), 5695–5719.

Nikolaidis R. 2002. Observation of geodetic and seismic deformation with the Global Positioning System, *Dissertation*, University of California, San Diego.

Nyst M. and Thatcher W. 2004. New constraints on the active tectonic deformation of the Aegean, *J. Geophys. Res.*, 109(B11406), doi:10.1029/2003JB002830.

Reilinger R., McClusky S., Vernant P., Lawrence S., Ergintav S., Cakmak R., Ozener H., Kadirov F., Guliev I., Stepanyan R., Nadariya M., Hahubia G., Mahmoud S., Sakr K., ArRajehi A., Paradissis D., Al-Aydrus A., Prilepin M., Guseva T., Evren E., Dmitrotsa A., Filikov S.V., Gomez F., Al-Ghazzi R.and Karam G. 2006. GPS constraints on continental deformation in the Africa-Arabia-Eurasia continental collision zone and implications for the dynamics of plate interactions, *J. Geophys. Res.*, 111(B05411), doi:10.1029/2005JB004051.

Van Dam T., Wahr J., Milly P.C.D., Shmakin A.B., Blewitt G., Lavallee D. and Larson K.M. 2001. Crustal displacements due to continental water loading, *Geophys. Res. Lett.*, 28, 651–654.

Williams S.D.P., Bock Y., Fang P., Jamason P., Nikolaidis R., Prawirodirdjo L., Miller M. and Johnson D.J. 2004. Error analysis of continuous GPS position time series, *J. Geophys. Res.*, 109(B03412), doi:10.1029/2003JB002741.

Zhang J., Bock Y., Johnson H., Fang P., Williams S., Genrich J., Wdowinski S. and Behr J. 1997. Southern California permanent GPS geodetic array: error analysis of daily position estimates and site velocities, *J. Geophys. Res.*, 102, 18035–18055.